


2016

Recycling wind turbine blade composite material as aggregate in concrete

Tyler Robert Fox
Iowa State University

Follow this and additional works at: <https://lib.dr.iastate.edu/etd>

 Part of the [Civil Engineering Commons](#), and the [Industrial Engineering Commons](#)

Recommended Citation

Fox, Tyler Robert, "Recycling wind turbine blade composite material as aggregate in concrete" (2016). *Graduate Theses and Dissertations*. 15159.
<https://lib.dr.iastate.edu/etd/15159>

This Thesis is brought to you for free and open access by the Iowa State University Capstones, Theses and Dissertations at Iowa State University Digital Repository. It has been accepted for inclusion in Graduate Theses and Dissertations by an authorized administrator of Iowa State University Digital Repository. For more information, please contact digirep@iastate.edu.

Recycling wind turbine blade composite material as aggregate in concrete

by

Tyler R. Fox

A thesis submitted to the graduate faculty
in partial fulfillment of the requirements for the degree of

MASTER OF SCIENCE

Major: Industrial and Manufacturing Systems Engineering

Program of Study Committee:

Frank Peters, Co-Major Professor

Sri Sritharan, Co-Major Professor

Peter Taylor, Co-Major Professor

Iris Rivero

Iowa State University

Ames, Iowa

2016

Copyright © Tyler R. Fox, 2016. All rights reserved.

TABLE OF CONTENTS

ACKNOWLEDGMENTS	iv
ABSTRACT.....	v
CHAPTER 1: INTRODUCTION.....	1
1.1 Literature Review	3
CHAPTER 2: EXPERIMENTATION	9
2.1 Methodology.....	9
2.2 Phase 1	13
2.3 Phase 2.....	15
2.4 Results	17
2.5 Discussion.....	23
CHAPTER 3: ECONOMIC ANALYSIS	33
3.1 Assumptions	34
3.2 Cost avoidance for sending wind turbines to landfill	35
3.3 Cost avoidance for obtaining limestone coarse aggregate	36
3.4 Cost avoidance for transporting aggregate	37
Cost of producing composite aggregate from wind turbines.....	38
CHAPTER 4: ENVIRONMENTAL IMPACT	40
4.1 Recycling vs landfilling vs incineration of composite material	40
4.2 Life Cycle Analysis	41

CHAPTER 5: SUMMARY AND CONCLUSIONS	45
5.1 Summary.....	45
5.2 Conclusions	46
REFERENCES	48
APPENDIX A: RAW DATA	52

ACKNOWLEDGMENTS

I would like to thank several organizations and individuals that assisted with this study by providing information, supplies, and research. First, Vermeer Corporation for providing insight and guidance when determining possible equipment to use for producing the composite aggregate. Second, TPI Composites for providing the composite material. Third, undergraduate research assistants Brent Chuck, Michael Hoffer, Alicia Guzman-Guierrez, and Brandon Landowski for their efforts put forth in procuring information and resources. Fourth, Robert Steffes and the Portland Cement Laboratory for their guidance on experiment operations. Finally, Warren Straszheim and the Material Analysis Research Laboratory for assistance with the scanning electron microscope and sample analysis.

ABSTRACT

This study investigates the beneficial reuse of composite material from wind turbine blades as aggregate in concrete pavement. The thesis is divided into three parts including an experiment, economic analysis, environmental impact study. An economic analysis revealed that the cost to process composite aggregate from wind turbine blades would need to be less than a value of \$62.72 per ton of composite aggregate to be financially feasible. The environmental impact study conducted a life cycle analysis (LCA) which favored the practice of recycling the composite aggregate based on a CO₂ emission avoidance on 2.3 lb (1.0 kg) per ton of composite aggregate produced.

The experiment included pretests to determine the appropriate size and volume fraction of composite aggregate necessary to maintain a minimum of 4000 psi compressive strength. Following pretest, the full experiment consisted of an ASTM C39 compression test and ASTM C496 split tensile test using a Test Mark CM-4000 SD machine, ASTM C157 shrinkage prism test using CDI Logic™ ALG gage, and a final corrosion test. Samples were cured in two environments of 100% humidity fog room and a calcium hydroxide bath at 160F (70C). These samples were tested at 7, 28, and 90 days. A maximum compression and tensile strength of 6,318 psi (43.6 MPa) and 578 psi (3.1 MPa) was observed in the humidity cured samples which was significantly higher than those stored in the hot bath. For the ASTM C157 test, hot bath samples yielded between 0.27 and 0.33% expansion which was approximately ten times higher than those in the fog experiment. Finally, a weight gain due to water absorption of 1.66% and 0.49% in the composite aggregate and limestone aggregate respectively was seen. In general, this study supports the use of composite material from wind turbine blades as aggregate in concrete.

CHAPTER 1: INTRODUCTION

Major strides have been made in the realm of renewable energy in the past 30 years. Wind energy is a shining example of these renewable energy sources. Wind energy supplied nearly 5% of the global electricity demand in 2014 [1]. The International Energy Agency predicts it will continue to grow and supply between 15% and 18% of the global electricity by 2050 [2]. The impact in the US is even larger with the expectation that wind energy will provide 20% of the nation's electrical demand by 2030 and 35% by 2050 [3]. This demand is expected to be met in two ways. First, with an increase in efficiency and average rated capacity of each turbine. This has already been seen as the average rated capacity has increased as well from 1.6 MW and 3MW in 2008 to 1.8 MW and 4 MW in 2012 for onshore and offshore turbines respectively [2]. The second is by transforming current locations with limited to no wind energy production potential into functioning wind sites by increasing the hub height of a tower to capture the wind potential at higher altitudes. In fact, a hub height of 459 ft (140 m) is expected to have a 67% increase in wind potential compared to the current 262 ft (80 m) hub height [4]. This increase in hub size will also directly relate to an increase in blade size as well [5].

Although wind energy is growing and the number of turbines is increasing each year, original turbines erected in the late 80s and early 90s are nearing the end of their lives, and those installed after 2000 will be reaching their end of life soon. The end-of-service-life [EOSL] is assumed to occur when a [wind turbine] has reached its designed life expectancy (20-30 years), cannot perform its function because of failure or fatigue, or no longer satisfies the needs or expectations of a user [6].

This EOSL wind turbine scenario has begun to raise the question regarding what needs to be done with these EOSL turbines. Recycling solutions have already been found for many of the

components of the decommissioned wind turbines. One major component with an inadequate EOSL solution is the turbine blades. By 2034, it is predicted that 248,020 tons (225,000 tonnes) of rotor blade material will need to be recycled annually worldwide [7]. The current solution of landfilling turbine blades will only serve as a temporary fix due to space constraints and landfill regulations.

Some areas will start to see these effects of this EOSL scenario sooner than others. As discussed prior, some locations currently have limited to no wind energy potential. However, one state which will see the full force of these issues is Iowa. Iowa is ranked in the top three states for installed wind capacity behind Texas and California. Iowa's wind capacity will continue to grow with 75% of the land being suitable for wind energy development leading to a total wind capacity of 570,000 MW [8]. This growth is already in motion as the Iowa Wind Energy Association has stated it plan to bring Iowa from its current installed capacity of 5,710 MW to 20,000 MW by 2030 [8]. With the large growth potential, Iowa is an excellent location to begin answering questions surrounding EOSL solutions for wind turbine blades. Several alternative methods are starting to be explored including thermal and mechanical recycling.

This study focuses on three different aspects of the mechanical recycling processes of using composite material as aggregate in concrete for pavement. It is an expansion upon the preliminary testing done by undergraduate researcher Michael Hofmeister at Iowa State University discussed later. The study first looks at the physical properties in concrete such as compressive strength, shear strength, and shrinkage coupled with a corrosion test to determine the long term effects of concrete on the composite aggregate. Second, an economic analysis was performed to determine the viable cost for producing the composite aggregate. Finally, an environmental impact study was conducted. The following will shine light on the idea of using

composite material from wind turbine blades as aggregate in concrete and discuss the viability of this EOSL solution.

1.1 Literature Review

Prior to diving into testing, economic analysis, and environmental impact, a review of previous work was conducted. This review covered general recyclability of wind turbines, legislation and landfill concerns driving the need for the recycling of wind turbine blades, additional attempts to recycle wind turbine blades, and potential issues with using the composite material as aggregate in concrete.

1.1.1 General Recyclability

To understand the need to focus on recyclability of the wind blades, a general knowledge of current wind turbine recycling is needed. It is common practice to recycle portions of a wind turbine such as the tower, gearbox, and hub which contain large quantities of steel. In fact, as much as 80% of the total weight of a wind turbine can be reprocessed and repurposed [9]. Steel, aluminum, and copper comprise a majority portion of this 80%. This is more clearly shown in **Table 1** created by the Princeton Energy Resources International which contains a breakdown of the materials used as a percentage of weight for major component [10]. These materials are commonly recycled and have been for decades. Many experts believe over 90% of these metals can be recycled [11]. In addition to the metals being recycled, the tops of the foundations are removed and the remaining portion is covered with soil.

Table 1: Percentage of materials used in current wind turbine components [10]

Component/material (% by weight)	Pre-stressed Concrete	Steel	Aluminum	Copper	Glass Reinforced Plastic
Rotor					
Hub		100			
Blades		5			95
Nacelle		80	3 - 4	14	1
Gearbox		98	2	2	
Generator		65		35	
Frame, Machinery, and Shell		85	9	4	3
Tower	2	98			

Although much of a wind turbine can be recycled, identifying appropriate methods of recycling the blades is needed. The blades contain some recyclable materials; however, they are largely comprised of fiberglass composite material. The blades and production waste of components are responsible for the majority of wind turbine waste to landfill [12]. Recycling the composite material can be difficult due to the complex material compositions, cross-linked nature of the thermoset resins, and logistical problems encountered by their size [13]. Overall, increased technological improvements in turbine recycling are required for optimum recyclability to occur [14].

1.1.2 Legislation and Landfilling

Currently, the most economic form of disposal for many municipal solid wastes is landfilling [15]. This holds true for EOSL wind turbine blades as well. Landfills do have a negative environmental impact on many things including potential health hazards, fires and explosions, vegetation damage, unpleasant odors, landfill settlement, ground water pollution, air pollution, and global warming [16]. Although landfilling is the most economical choice in many

cases, these negative impacts will continue to push toward the reduction in landfill usage as the number of EOSL wind blades continues to grow.

The process of finding the new EOSL options for many products has already begun in the EU. As of 1999, the EU launched its landfill directive to reduce the level of biodegradable waste being landfilled. A more specific piece of legislation can be seen in Germany. This legislation enforced a ban on municipal solid waste in landfills [13].

1.1.3 Additional Attempts

Efforts have begun on multiple fronts to determine methods of recycling the composite material from wind turbine blades. Thermal recycling is being explored in multiple ways including pyrolysis, microwave pyrolysis, and fluidized bed thermal process. Pyrolysis is not a novel method of recycling. It has been used on composite plastic components in the past to produce fuel and provide energy for additional pyrolysis operations [17]. Pyrolysis of the blade material will burn off the resin and leave recyclable glass fibers. In addition to pyrolysis, studies have been performed to determine the effects of microwave pyrolysis. Mechanical tests of composite samples containing 25% recycled fiber by weight from microwave pyrolysis have relatively good mechanical properties [18]. Microwave pyrolysis may reduce the energy input compared to normal pyrolysis [19]. This would help retain some mechanical properties of the glass fibers lost during pyrolysis. An additional method that may retain the mechanical properties and value of material is the fluidized bed thermal process. The composite material sits in fine grain particles such as sand which are fluidized using air. The process is heated and organic particles are volatilized with the polymer matrix while inorganic solids such as metal inserts sink and may be removed [20].

Mechanical processing has also been used in the past. These processes are typically done by hammer milling, grinding, or shredding to reduce the size of the composite material. These create filler materials such as powder and can be used as a substitute for calcium carbonate filler in new sheet molding compound (SCM) or bulk molding compound (BMC) and potential reinforcements in more fibrous BMC [21]. The lower density of the composite compared to calcium carbonate provides the advantage of creating lighter SCM components. This advantage comes with drawbacks as well. One issue arises with recycled fillers as they often have different properties than conventional fillers [22].

Several European companies, Holcim AG/Geocycle and Zajohn, have combined efforts to determine alternative recycling possibilities and are striving to find the optimal recycling process for the blades. According to the European Wind Energy Association, no appropriate recycling method has been found. This is due to lack of adequate logistics solutions in addition to the environmental risks caused by dust and solvent emissions [23]. Holcim and Zajohn have devised a process in an attempt to overcome these obstacles. The blades are broken down into 11 yard (10 m) long transportable sized pieces at the turbine site using a mobile cutting device. To minimize emissions, the cutting site is humidified. These small pieces are then shipped by truck or train to the recycling plant where automated saws further cut the blades into 0.9 yard (1 m) long chunks. The chunks are then fed into a shredder where they are broken down to pieces less than 2 inches (50 mm) in length. The dust created from these operations is also bonded together to reduce environmental emissions [24]. These smaller chips and fibers are then used to create cement in a kiln. The useable thermal energy from a blade resin is 6.35 MJ/lb (14 MJ/KG) which is approximately half of hard coal and can be used as an energy substitute. Once burned, the ash

mixes with raw materials in the sintering zone in the cement kiln to be created into new cement [25].

Although Holcim and Zajohn have laid the ground work for recycling composite material in cement production, other options have yet to be thoroughly explored. Another solution to look into is recycling the composite waste materials and using it as aggregate in concrete. Preliminary work has been conducted by undergraduate researcher, Michael Hofmeister, at Iowa State University as initial tests for this option. Composite cubes between 0.25 and 0.5 inches (6.35 and 12.7 mm) were used to replace limestone aggregate. This resulted in finding the compressive strength decreases almost linearly with a total drop of approximately 70% compressive strength between 0%, 50%, and 100% aggregate substitution. Thin strips of composite material have also been shown to increase the strain values when compared to concrete samples with no composite material [26]. Additionally, Hofmeister examined the effects of pyrolyzed composite fibers between 1.00 and 1.25 inch (25.4 and 31.8 mm) at 1% by volume which yielded a 27% decrease in compressive strength, however, the pyrolysis was not controlled well resulting in fibers that contained residue from the resin.

Using recycled material as aggregate in pavement construction reduces the need for virgin or natural aggregates, preserves the environment, and saves landfill space [27]. A key advantage to using waste or recycled materials such as plastics or composite material in concrete is to help reduce the solid wastes being landfilled [28]. The results of previous studies showed that recycled materials (other than the composite material from wind turbine blades) can be incorporated into concrete without detrimental effects [29]. Many recycled wastes have been used in the past for aggregate in concrete including plastics, coal ash, rubber tyre, leather, mining industry wastes, and more [30].

1.1.4 Potential Issues

There are two major concerns when using a fiberglass composite as aggregate in concrete. The first is that the acidic properties of the concrete are known to deteriorate glass over time. The glass is also known to have slight negative effects on strength, workability, and freeze-thaw resistance [31]. Studies show that glass used as coarse aggregate causes the mechanical properties to decline as the volume fraction of glass aggregate increases [32]. This could lead to unstable concrete that needs to be replaced at more frequent intervals. Second, the ability of cement to bond with the resin and smooth surfaces of the composite material raises issues. This ability to bond depends on both adhered mortar quality and the amount of adhered mortar [33]. It has been shown that the smooth surface created by the resin in composite materials reduces the bond strength between cement and the composite material [34]. Generally, there is a fall in the 28-day compressive strength because of the weak interface between the glass aggregates and the hardened cement paste [35]. Although the pieces of composite aggregate contains glass fibers rather than chunks, these concerns were still taken into consideration throughout the study.

As wind energy grows, more and more studies will be conducted bringing new insights to the best EOSL location and recyclability of wind turbine blades. Each will encounter its own issues with economic justification, environmental issues, and uses. This thesis explores and addresses these issues for the recycling of composite material from wind turbine blades as aggregate in concrete.

CHAPTER 2: EXPERIMENTATION

2.1 Methodology

Before exploring the economic feasibility or environmental impact of using recycled composite material from wind turbine blades as aggregate in concrete, the question of if this composite material is capable of being used as an aggregate in concrete needs to be answered. To determine this, a study was conducted on the compressive strength, tensile strength, shrinkage, and corrosion of concrete containing composite aggregate and the composite aggregate itself.

2.1.1 Aggregate Creation

A method of creating the composite aggregate from wind turbine blades needed to be found prior to pouring the concrete samples used in this experiment. The composite material consisted of 1 part of Hexion EPIKURE™ Resin MGS RIMR 135 mixed with 30% part of EPIKURE™ Curing Agent MGS RIMR 1366 by weight and glass. The material used was donated by TPI Composite Inc. in Newton, IA and from Iowa State University's Wind Energy Manufacturing Lab in Ames, IA, but was essentially identical regardless of the source. It consisted of discarded test and scrap production components. Examples of this starting material can be seen in **Figure 1**.



Figure 1: Sample material provided by TPI

The curved samples provided both useable and non-useable material. Pieces deemed unusable were either too thin, ranging from 1/8-1/2 inch (3.2 – 1.3 cm) or were thicker than 1 inch (2.5 cm). No machine was found that was capable of creating the desired geometry

for the composite aggregate so a manual process was used. The ideal geometry is irregular shaped blocks with a rough surface and minimum dimensions between 0.5 inch (1.3 cm) and 1 inch (2.5 cm). This process was not possible using a manual process either so a compromise was found by using rectangular blocks with one to three rough sheared edges and three to five smooth, cut edges. The manual process to create this aggregate included a cutting and shearing method. First, the non-useable material needed to be separated from the useable material. To achieve this, several cutting operations were tried including band saw and sliding wet saw. A band saw was used but could only achieve a cutting speed of 20 inches per minute and the blade required replacement after approximately 150 inches of cutting. The sliding wet saw proved much more viable to cut the useable material from non-useable material. Once separated from the non-useable material, the useable material was cut into strips as seen in **Figure 2**. The strips were then sheared into the final aggregate pieces used in this study shown in **Figure 3**.

This process was very time consuming. In total, it took over 50 hours of labor to produce 183 lb (83 kg) of composite aggregate and often required multiple operators to manipulate the



Figure 2: Strips of material cut by wet saw



Figure 3: Composite aggregate created using manual process

larger sheets of composite material and cut them down to a manageable size. This cutting operation would not be a practical way to produce composite aggregate in mass quantities due to the time, labor, and smooth finish created on the material.

The issues seen with the smooth surfaces were partially counteracted by the shearing process on the strips. The orientation at which the composite material was sheared had a large impact on aggregate production. When shearing with the fibers, the composite material shreds and split into many fibrous pieces. Shearing against the fiber creates a cleaner shear while still having a rough surface finish desired of aggregate material. The result of shearing with and against the fiber of the composite material can be seen in **Figures 4 and 5**, respectively. The images from left to right are the front, top and right sides of composite aggregate.

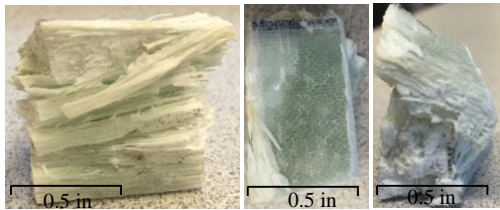


Figure 4: Front, Top, and Right views of shearing with the fiber

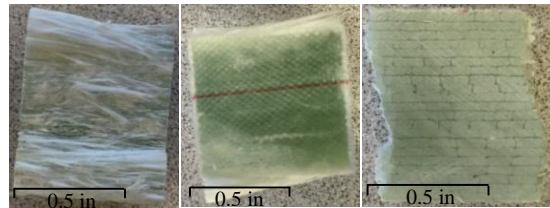


Figure 5: Front, Top, and Right views of shearing against the fiber

Once the composite aggregate was created, it was put through a sieving shaker with screen sizes of 1.5, 1, 0.75, 0.5, and 0.375 inch (3.8, 2.54, 1.9, 1.3, and 1 cm) along with sieve #4 and #50. The aggregate found on the screen sizes 0.5 and 0.75 inch (1.3 and 1.9 cm) was used in this study. Other methods of hammer milling, crushing, and chipping were explored to determine a more efficient method of producing the composite aggregate. The crushing operation was attempted using a rock crusher shown in **Figure 6**. Hammer milling and crushing were ineffective in breaking down the composite material. Those put through the hammer mill were slightly dented but not broken. Those that went through the rock crusher were shredded similar

to the strips that were sheared with the fibers. Samples of aggregate put through the rock crusher and chipper can be seen in **Figures 7 and 8**, respectively. No pictures of samples put through the hammer mill were taken. Of these three options explored, chipping showed the most promising results creating long strips and slabs of the material. However, they were still unusable due to the shredding and inadequate geometry that occurred. In addition to being the most promising, it also was significantly faster. Designing and creating a technology to produce the composite aggregate while maintaining economic feasibility could pose a problem.



Figure 6: Rock crusher



Figure 7: Samples from rock crusher



Figure 8: Samples from Chipper

2.1.2 Mixture Proportions

Once the aggregate was created, the mixture proportions of concrete samples were determined. The water to cement ratio used through the experiment was constant at 0.45. The fine aggregate was local river sand and accounted for 42% of the total weight of all the aggregate used. Portland cement was used in this experiment. The natural fine and course aggregate came from local river sand and limestone came from the Ames Mine in Ames, IA. The composite aggregate was broken up into two sizes, 1 and 0.5 inch (2.5 and 1.3 cm) cubes. Due to a difference in densities, the ratio of composite to limestone aggregate was made by volume. At 3,071 lb/yd³, the composite material is over 25% less dense when compared to the 4,315 lb/yd³

(2,560 kg/m³) limestones aggregate. No additional chemicals or air were added to any of the samples during this experiment. Additionally, it should be noted that samples in Phase 2 were created using two batches of concrete. Further breakdowns of the mixture proportions for each section of the experiment can be seen in **TABLE 2**.

Table 2: Mixture proportions for concrete used in this study

Mixture proportions for concrete in lbs/yd ³ (KG/m ³)							
Phase	Sample	Cement	Water	1" CA	1/2" CA	LA	FA
Phase 1 Size	Control	254.3 (150.8)	114.4 (67.9)	0.0 (0.0)	0.0 (0.0)	699.8 (415.0)	506.7 (300.5)
	1/2" CA	254.3 (150.8)	114.4 (67.9)	0.0 (0.0)	240.5 (142.6)	349.9 (207.5)	506.5 (300.4)
	50-50 CA	254.3 (150.8)	114.4 (67.9)	120.3 (71.3)	120.3 (71.3)	349.9 (207.5)	506.5 (300.4)
	1" CA	254.3 (150.8)	114.4 (67.9)	240.5 (142.6)	0.0 (0.0)	349.9 (207.5)	506.5 (300.4)
Phase 1 Volume	Control	254.3 (150.8)	114.4 (67.9)	0.0 (0.0)	0.0 (0.0)	699.8 (415.0)	506.7 (300.5)
	25% CA	254.3 (150.8)	114.4 (67.9)	120.5 (71.4)	0.0 (0.0)	525.8 (311.8)	507.5 (301.0)
	37.5% CA	254.3 (150.8)	114.4 (67.9)	180.5 (107.0)	0.0 (0.0)	437.5 (259.4)	506.8 (300.5)
	50% CA	254.3 (150.8)	114.4 (67.9)	240.5 (142.6)	0.0 (0.0)	349.9 (207.5)	506.5 (300.4)
Phase 2	ASTM C 39	254.3 (150.8)	114.4 (67.9)	156.4 (92.7)	0.0 (0.0)	472.3 (280.1)	506.6 (300.4)
	ASTM C 157	254.3 (150.8)	114.4 (67.9)	156.4 (92.7)	0.0 (0.0)	472.3 (280.1)	506.6 (300.4)
	ASTM C496	254.3 (150.8)	114.4 (67.9)	156.4 (92.7)	0.0 (0.0)	472.3 (280.1)	506.6 (300.4)

*CA - Composite aggregate

*LA - Limestone aggregate

*FA - Fine aggregate

2.2 Phase 1

The experiment in this study consisted of two phases, Phase 1 and Phase 2. Phase 1 was made of two pretests. The first pretest was used to determine the appropriate composite aggregate size. The second was a test to determine the volume fraction of composite aggregate to be used. These results of Phase 1 were then used to determine the mix proportions for Phase 2.

2.2.1 Pretest 1: Composite Aggregate Size

To determine the mixture proportions for Phase 2, several pretests were conducted. The first pretest determined the appropriate size of the composite aggregate by performing an ASTM C39 compression test using a Test Mark CM-4000 SD on 4x8 inch (10.1 x 20.3 cm) cylinders. All cylinders used throughout this study were of the same dimensions. In total, four types of mixture proportions were used in this pretest, and three cylinders were made from each type for a total of twelve cylinders. The first type was the control cylinders. These cylinders consisted of

100% limestone aggregate. Type two, ½” CA, contained 50% 0.5 inch (1.3 cm) composite aggregate and 50% limestone aggregate. The third type, 50-50 CA, consisted of 25% 0.5 inch (1.3 cm) composite aggregate, 25% 1 inch (2.5cm) composite aggregate, and 50% limestone aggregate. The final type, 1” CA, used 50% 1 inch (2.5 cm) composite aggregate and 50% limestone aggregate. The breakdown of the full mixture proportions used in Phase 1 can be seen in the Phase 1 Size section of **Table 2**.

Once the concrete was mixed it was poured into molds. Samples were set to hydrate for 24 hours. After 24 hours, they were placed in a fog room with 100% humidity for seven days. After the seven days in the fog room, all cylinders were removed to be tested. The ASTM C39 compression test was performed with the twelve cylinders to determine the strength difference between the different types of mixture proportions. No minimum threshold psi was set for this test.

2.2.2 Pretest 2: Composite Aggregate Volume

The second pretest performed was a volume test. The goal of this pretest was to reach a threshold of 4,000 psi (27.6 MPa). Based on the results discussed later from the composite aggregate size pretest, a maximum dimension of 1 inch composite aggregate size was chosen to be used in the volume test. Three separate volumes of composite course aggregate tested include 25%, 37.5%, and 50%. The remaining 75%, 66.5%, and 50% respective course aggregate quantities were filled with limestone. There was no need to test samples with a composite aggregate volume fraction above 50% because the size pretest, which contained 50% composite aggregate by volume, did not yield a psi strength greater than 4,000 (27.6 MPa).

The volume pretest was conducted in similar fashion as the composite aggregate size pretest. Four types of mixture proportions were used in the volume pretest, and three cylinders

were made from each type for a total of twelve cylinders. The first type was the control cylinders. These cylinders consisted of 100% limestone aggregate. Type two, 25% CA, contained 25% 1 inch (2.5 cm) composite aggregate and 75% limestone aggregate. The third type, 37.5% CA, consisted of 37.5% 1 inch (2.5 cm) composite aggregate and 62.5% limestone aggregate. The final type, 50% CA, used 50% 1 inch (2.5 cm) composite aggregate and 50% limestone aggregate. The breakdown of the full mixture proportions used in Phase 2 can be seen in the Phase 2 Volume section of **Table 2**.

Once the concrete was mixed it was poured into the molds. Samples were set to hydrate for 24 hours. After 24 hours, they were placed in a fog room with 100% humidity for seven days. After seven days in the fog room, the cylinders were removed and the ASTM C39 compression test was performed. The results of this test are shown and discussed later in the Results and Discussion sections. One cylinder of each sample type was kept for observations purposes in both Pretest 1 and Pretest 2.

2.3 Phase 2

The size and volume tests conducted in Phase 1 determined the mixture proportions for Phase 2. Phase 2 of the experiment consisted of four different tests. These tests include the ASTM C39 compression test, ASTM C496 split tensile test, ASTM C157 shrinkage test, and a corrosion test. The compression test, split tensile test, and shrinkage test all contained 32.5% composite aggregate and 67.5% limestone aggregate with an approximate aggregate size of 1 x 1 x 1 inch.

These samples were simply the aggregate pieces themselves and were not part of concrete samples. The corrosion test was performed by placing both composite and limestone aggregate samples in a calcium hydroxide bath at 160F (70C). The calcium hydroxide was used

to mimic the effects of cement to show how the composite and limestone aggregates would react. The breakdown of the full mixture proportions used can be seen in the Phase 2 section of **Table 2**

In total, 48 4x8 inch (10.1 x 20.3 cm) cylinders were poured in addition to six 4x4x11 inch (10.1x10.1x30 cm) prisms. They were set to cure for 24 hours. After 24 hours, they were broken out of their molds. Half of the cylinders and half of the prisms were placed in a fog room with 100% humidity. The other half of the samples were placed in a hot bath containing calcium hydroxide at 160F (70C). Additionally, when the cylinders and prisms were placed in the calcium hydroxide, eight samples each of the composite and limestone aggregate were placed in the calcium hydroxide bath for the corrosion test.

The ASTM C39 compression test and C496 split tensile test were conducted on three cylinders each from both curing conditions (humidity room and hot bath) after seven, 28 and 90 days of curing. This series of tests consumed 36 cylinders, the remainder of the cylinders were kept for future observational purposes. The ASTM C157 shrinkage prism test and the corrosion tests were performed after seven, 28, and 90 days as well. Prisms stored in the hot bath were left to cool for 30 minutes. During this time, the shrinkage test was performed on the prisms stored in humidity room at 70F (21C), and the corrosion test samples were weighed to determine mass change. After the 30 minutes, the hot bath samples were then measured.

2.4 Results

2.4.1 Phase 1

2.4.1.1 Results of the size test to determine optimal size.

The ASTM C39 Compression test yielded the following results, which were then used to determine the optimal size of composite aggregate to use for the mixture proportions of the volume pretest for Phase 1 and all of Phase 2. The control samples broke at an average of 5,882 psi (40.5 MPa) which was significantly higher than those that contained composite aggregate. When comparing the three sample types containing composite aggregate, it does not appear that the different sized aggregate had an effect on the average compressive strength. With no difference found, the 1" CA size was chosen for the volume pretest and Phase 2. **Figure 9** provides a numerical view of the results from this pretest. Additionally, a breakdown of these numbers can be seen in **Table A1** in the Appendix. There is no significant statistical difference between the ½" CA, 50-50 CA, and 1" CA. All three types of composite aggregate samples were statistically different from the control sample.

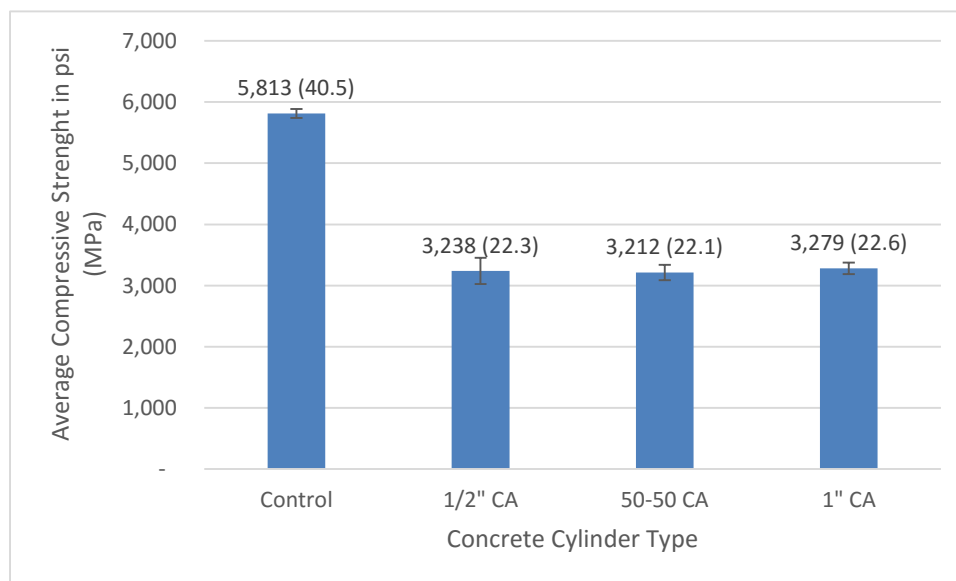


Figure 9: ASTM C39 Compression test for composite size

2.4.1.2 Results of the volume test using optimal size to determine optimal volume.

The ASTM C39 compression test yielded the following results for the volume pretest. The control samples broke at an average of 5,813 psi (40.5 MPa). The 25, 37.5, and 50 percent composite aggregates broke with an average psi 4,531, 3,634, and 3,212 (31.2, 25.0, and 22.1 MPa) respectively. These results appear to have a linear relationship with R^2 value of 0.95 and are displayed in **Figure 10**. A further analysis of these numbers can be seen in **Table A2** in the Appendix. These values were used to determine the optimal volume of composite aggregate for the mixture proportions of Phase 2. This test was used to determine the volume fraction of composite aggregate that would achieve 4,000 psi (27.6 MPa).

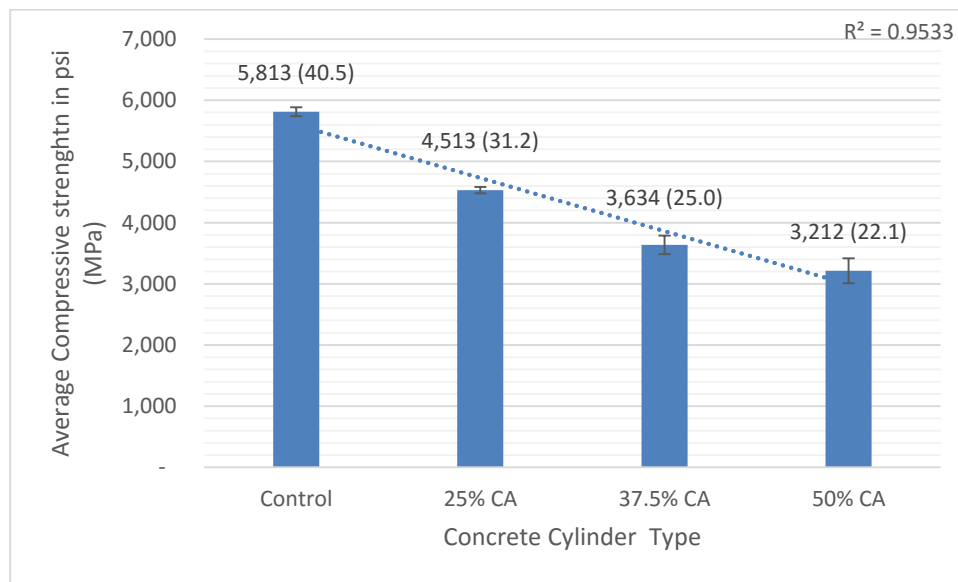


Figure 10: ASTM C39 compression test for composite volume

To determine what this volume fraction was, the following equation was used:

Equation 1:

$$OV\% = 25\% + \frac{P_{OV} - P_{25\% CA}}{P_{37.5\% CA} - P_{25\% CA}} (37.5\% - 25.0\%);$$

where $OV\%$ is the optimal volume fraction needed to achieve 4,000 psi (40.5 MPa), P_{OV} is the pressure at optimal volume fraction, $P_{25\% CA}$ is the pressure at 25% composite aggregate, and $P_{37.5\% CA}$ is the pressure at 37.5% composite aggregate. Based on *Equation 1*, a volume fraction of 32.3% composite aggregate is required to achieve a 4,000 psi (40.5 MPa). For the purposes of this study, the volume fraction 32.5% composite aggregate and 67.5% limestone aggregate was used in the mixture proportions in Phase 2 of the experiment.

2.4.2 Phase 2

2.4.2.1 Results of ASTM C39 compression test

Based on the optimal size and volume of composite aggregate determined in Phase 1, the Phase 2 tests were produced. The results of the ASTM C39 compression test are shown in **Figure 11**. At each of the three cure times, the samples stored in the 100% humidity environment had higher compressive than those stored in the hot bath. However, as the compressive strength increased with time for those in the 100% strengths humidity, the strength decreased for those in the hot bath.

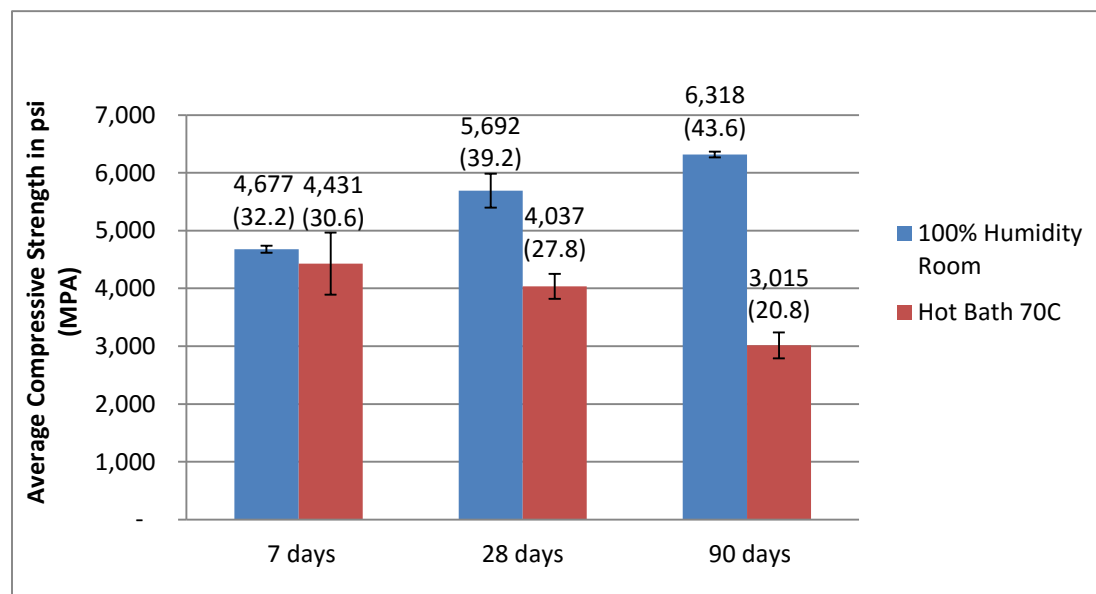


Figure 11: ASTM C39 compression test for different curing environments with cylinders containing 32.5% composite aggregate

2.4.2.2 Results of ASTM C496 split tensile test

Similar to the results seen in the ASTM C39 compression test, the 100% humidity room samples in the ASTM C496 tensile test show continuous strength increases over time. Likewise, the hot bath samples see a decrease in their tensile strength. The results of the split tensile test are shown in **Figure 12**. Unlike those found in the compression test, the samples at 90 days for the split tensile test show only a slight increase or decrease in tensile strength compared to that obtained 28 days, which implies continued curing may not have a large effect on tensile strength.

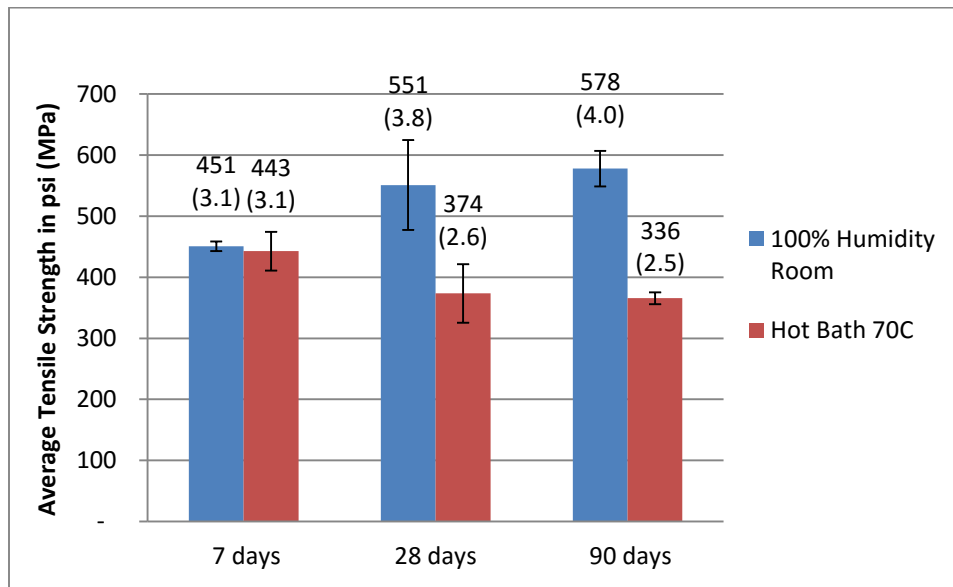


Figure 12: ASTM C496 split tensile test for different curing environments with cylinders containing 32.5% composite aggregate

2.4.2.3 Results of ASTM C157 shrinkage prism test

The ASTM C157 shrinkage prism test showed interesting results. As shown in **Figure 13**, those in the fog room showed a near zero change throughout the 90 day curing cycle.

Changes in fog room samples range from 0.02-0.03%. Those stored in the hot bath displayed

significantly more expansion over the entire curing cycle although they started with only slightly larger values than the fog room at the seven days measurement. Hot bath samples ended with expansion values between 0.27% and 0.33%. A clearer representation of the expansion from each sample can be seen in **Table 3**.

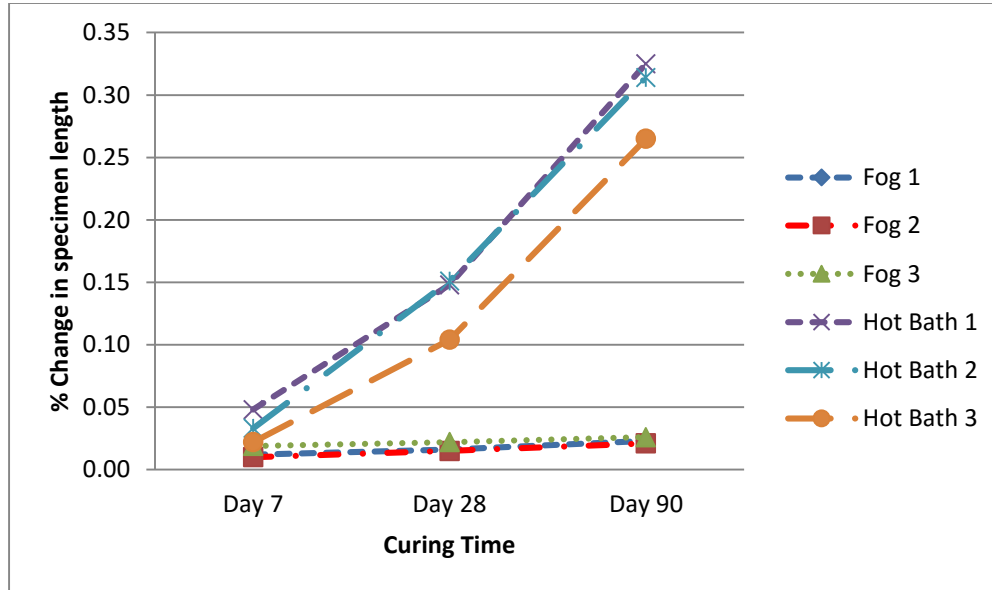


Figure 13: ASTM C157 shrinkage prism test for different curing environments with cylinders containing 32.5% composite aggregate

Table 3: Percent change in specimen during ASTM C157 test with cylinders containing 32.5% composite aggregate

Curing Environment	Fog Room			Hot Bath		
Sample #	1	2	3	1	2	3
Day 7	0.01	0.01	0.02	0.05	0.03	0.02
Day 28	0.02	0.01	0.02	0.15	0.15	0.10
Day 90	0.02	0.02	0.03	0.33	0.31	0.27

2.4.2.4 Results of corrosion test

The corrosion test was different from the other tests performed in this study. This test did not involve concrete. Instead, aggregate samples were stored in calcium hydroxide to mimic the

pH environment found in concrete to determine its effects on both the composite and limestone aggregates. The calcium hydroxide was used to mimic the acidic environment seen in cement. Similar to the shrinkage test, the corrosion test showed surprising results. The objective was to measure mass loss due to corrosion; instead, mass gain likely due to water absorption was observed. The composite samples showed weight gains of more than three times the amount of the limestone aggregate at the age of 90 days. In the first seven days of soaking, limestone samples gained an average of 0.45% of their total weight. Composite samples showed almost double that weight gain with an average of 0.83%. The weight gain for both composite and limestone slows after the first seven days. Composite samples would double their initial seven day weight gain to end with 1.66% weight gain at the end of 90 days. Limestone aggregate shows a much less drastic change, ending the 90 day curing cycle with 0.04% increase from its initial seven day weight for a final average weight gain of 0.49%. The average weight gain comparison between the limestone and composite aggregate can be seen in **Figure 14**. The actual weights of each aggregate sample can be found in **Table A3** and **Table A4** in Appendix A.

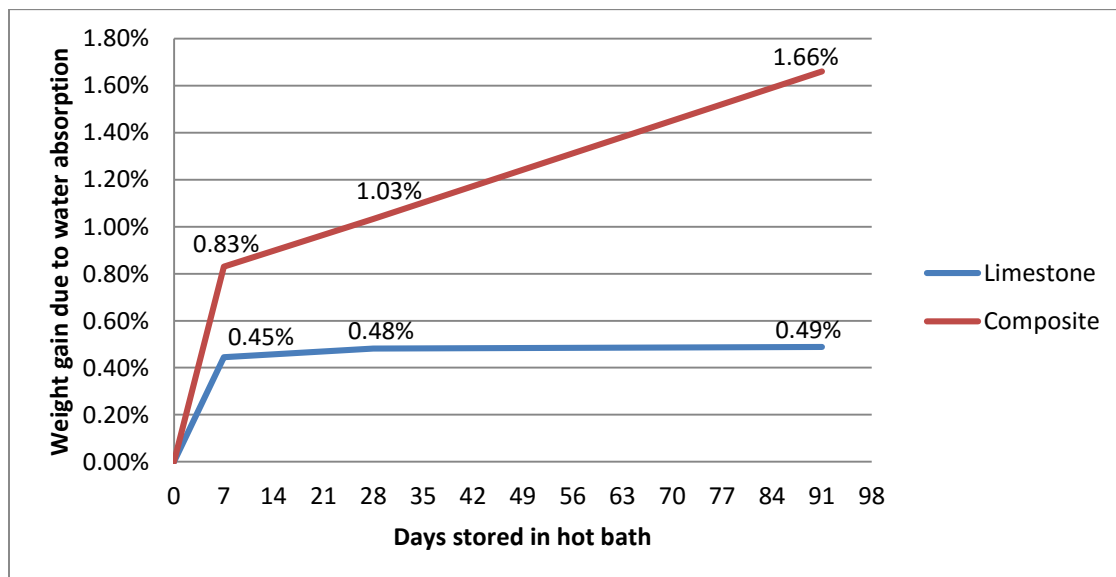


Figure 14: Average weight gain for composite and limestone aggregates

2.5 Discussion



With all the test results in mind, taking a deeper analysis will be necessary determine whether or not the composite material from wind turbine blades is a suitable aggregate for concrete. To start, the effects of the aggregate size and shape must be addressed.

Smaller composite aggregate samples were expected to yield higher compressive strengths due to the reduction in shear plane size between the surface of the composite aggregate and mortar. However, no statistical difference between the different aggregate sizes ($\frac{1}{2} \times \frac{1}{2} \times$

$\frac{1}{2}$ and $1 \times 1 \times 1$ inch [1.27 x 1.27 x 1.27 cm and 2.54 x 2.54 x 2.54 cm])

were found. Although the smaller shear plane size between the aggregate and mortar did not cause a difference in compressive strength, each sample preferentially fractured along the smooth surfaces of the composite aggregate as seen in **Figure 15**. This was expected because unlike limestone aggregate which is irregular in geometry, the composite aggregate pieces were rectangular prisms. This geometry is thought to have caused a lower compressive strength since irregularly-shaped coarse aggregates slightly increase the strength generated at the aggregate/mortar interface [36]. A solution to this issue may be found in irregularly-shaped geometry with increased surface roughness on smooth edges of the composite material. If a process existed to create composite aggregate to have an irregularly-shaped geometry and increase the surface roughness, similar to limestone aggregate, the overall strength of these

samples would increase. An attempt to create such geometry and increase the surface roughness to improve the bond strength between the mortar and composite aggregate face was made using a rock crusher. It was unsuccessful due to the composite material splitting and cracking. This cracking creates new interior surfaces that must be covered and bonded to the mortar, thus increasing the amount of mortar needed. For example, if a composite aggregate has six sides and cracks down the middle, now there is a 33% increase in surface area exposed.

While the composite aggregate had the disadvantage of cracking along its smooth sides, each sample broke through the limestone aggregate during testing. Breaks through the composite aggregate were not observed. Further research is needed to determine if irregular-shaped composite aggregate and rougher surface finish on smooth sides of composite aggregate would result in the composite aggregate fracturing, or if the bond strength between the composite aggregate and mortar would remain the point of failure.

The aggregate size test discovered the threshold of 4000 psi (40.5 MPa) could be reached using composite aggregate. The volume test was designed to determine the maximum volume fraction of composite aggregate that would produce the 4000 psi (40.5 MPa). This threshold was found to be 32.5% composite aggregate and 67.5% limestone aggregate at seven days with the expectation that it would continue to increase as the concrete cured.

If the course aggregate was 32.5% composite aggregate, there is a significant weight advantage to using the composite aggregate in addition to limestone. The substitution of composite aggregate for limestone aggregate would result in almost a 5% decrease in overall weight of the concrete due to the density difference between the two materials.

Although the decrease in weight is certainly an advantage to using the composite material, there appeared to be negative effects of using the composite material as well. During

the curing stage of the experiment, samples stored in the hot bath displayed external cracking. As the experiment progressed from seven days of curing, to 28, and 90 days, the cracking continued to propagate throughout the hot bath samples. These cracks appeared to have directly affected how the samples broke. When the ASTM C39 compression test was performed, the samples tended to break along the pre-existing cracks found on the hot bath samples. While cracks were very prevalent on the hot bath samples containing composite aggregate, no visible external defects were found on samples cured in the humidity room during any stage of the experiment. Examples of each of these conditions can be found in **Figures 16, 17, and 18** respectively.



Figure 16: Sample stored in fog room displays no sign of cracking



Figure 17: Cracking seen on samples stored in hot bath



Figure 18: Compressive failure along cracking caused by curing

There are several reasons this cracking was believed to have occurred. The first is thermal cracking, which may have occurred due to the prolonged exposure to an elevated temperature environment. The second is due to an alkali-silica reaction (ASR). Previous experiments have also shown that using glass as aggregate can cause sample strength reduction and excessive expansion due to the alkali-silica aggregate reaction [37]. This reaction can induce

pressure, expansion, and cracking of the aggregate and surrounding cement paste [38].

Additionally, heat is also known to speed up the alkali-silica reaction [39]. ASR appears in the form of a white efflorescence paste between the interface of the glass and mortar. When samples were removed from the hot bath, efflorescence appeared to be emerging from the cracks shown in **Figure 19**.

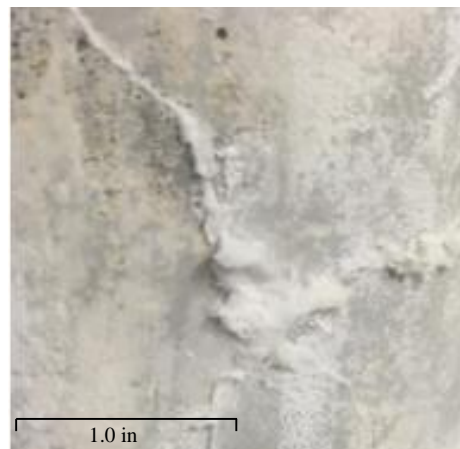


Figure 19: Efflorescence emerging from cracks in heat cured samples

A further analysis of the cracking was done to determine the true cause using a FEI Quanta-FEG 250 scanning electron microscope (SEM). A sample from each curing location, fog room and hot bath, were taken and a slice was cut out and polished to be analyzed. During this process several interesting things appeared. First, both samples showed cracking around the composite aggregate, limestone aggregate, the concrete paste as seen in **Figure 20**. This was intriguing because cracking was only expected to be seen in the hot bath samples. Second, porosity appeared near the edges of the composite aggregate shown in **Figure 21**. Third was a complete lack of bonding between the smooth edge of the composite aggregate and the mortar. Finally, there was no sign of ASR present in either sample. The lack of ASR came as a surprise, but may have been hindered by the resin in the composite material not allowing for significant exposure of glass to the mortar. This issue is discussed in more detail later.

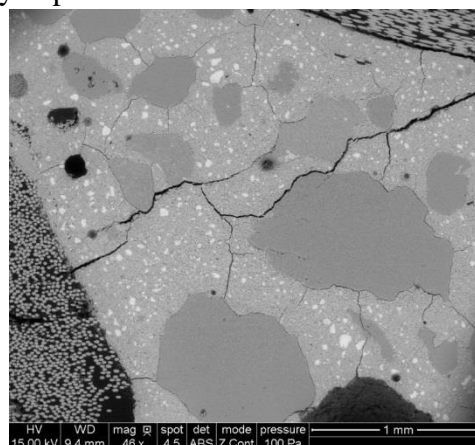


Figure 20: Cracking around both composite and natural aggregate

The cause of cracking around both the composite and regular aggregates and through the concrete paste appeared in both samples is unknown. It is believed that a change in dimensions in the composite aggregate caused this internal cracking to occur. It is unlikely that the change in dimension could have been caused by thermal expansion due to the appearance in both the fog room and hot bath samples. It is possible the cracking was induced by the vacuum chamber of the SEM. The most likely scenario is that the change came from water absorption by the composite aggregate causing it to swell and the mortar to crack.

The porosity was believed to be caused by water being absorbed by the composite aggregate. The SEM showed that these sections contained a lower amount of oxygen level compared to mortar around the limestone aggregate and throughout the concrete mixture. The lower oxygen levels indicate a lack of water present in these sections. The porosity was also found to be more significant along the sheared edges of the composite aggregate compared to the smooth edges. The fractured material and larger surface area from the sheared side is thought to have caused easier and more water absorption than a smooth side. An example of the porosity is shown next to the composite aggregate in **Figure 21**. Additionally, **Figure 22** shows the more extensive porosity along the sheared edge of a part.

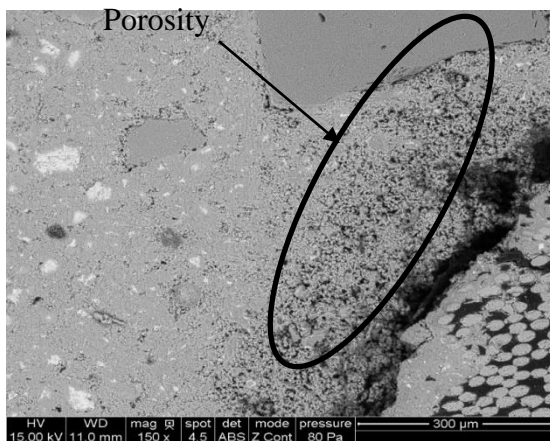


Figure 11: Porosity in the mortar-composite interface

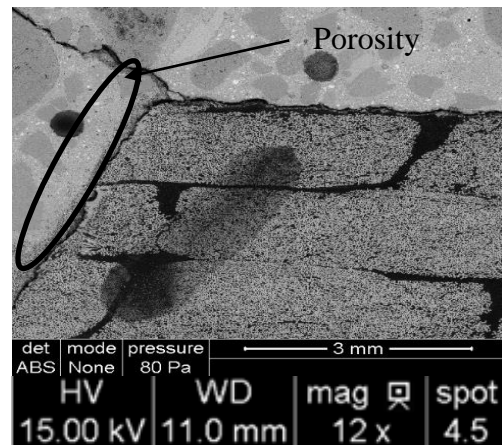


Figure 22: Higher amount of porosity along sheared edge of composite

In addition to porosity issues, there was a complete lack of bonding between the smooth edges of the composite aggregate. **Figures 23 and 24** show separation between the smooth edges of composite aggregate in the hot bath sample was significantly larger than that of the fog room samples. The hot bath gaps measured between 90 and 100 μm wide, while the fog room gaps were much smaller, at approximately 10 μm .

The smooth edge did show poor bonding; however, better bonding was seen along the sheared edges of the composite material. Some instances of no bonding occurred as shown in **Figure 25**. The better bonding observed along the sheared edges further supports the samples breaking along the smooth shear plane discussed earlier.

Although there was cracking that appeared, there were no signs of ASR inside either sample. Additionally, a small sample of the efflorescence found in the cracks was analyzed to determine if it was a result of an ASR. After further analysis, the efflorescence found in the cracks of the hot bath samples appeared to be calcium carbonate and

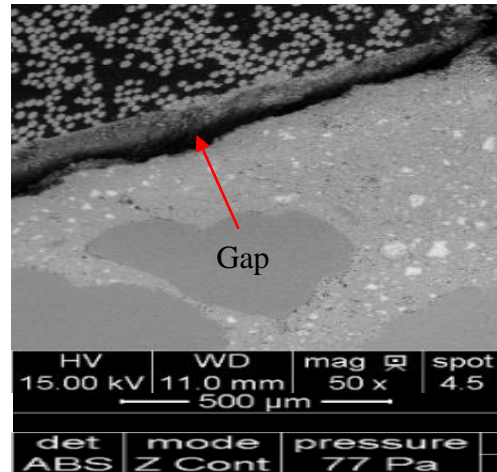


Figure 23: Hot bath smooth surface gap of 100 μm

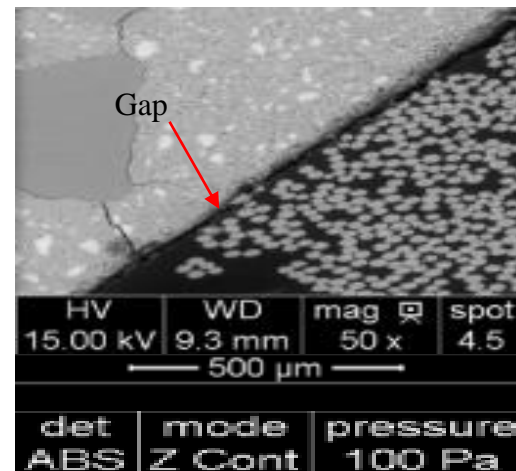


Figure 24: Fog room smooth surface gap of 10 μm

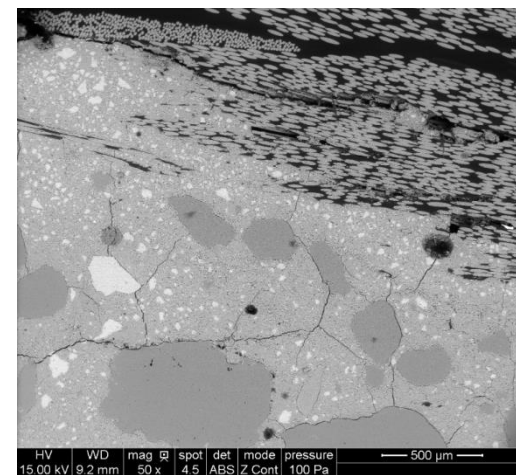


Figure 25: Sheared edge bonding between composite aggregate and mortar

magnesium hydroxide. Very low volumes of silica and no alkali-metals appear in the samples taken. This is believed to have been formed through reactions while the samples were being stored in the calcium hydroxide. A look at all the elements present in the efflorescence found can be seen in **Figure 26**.

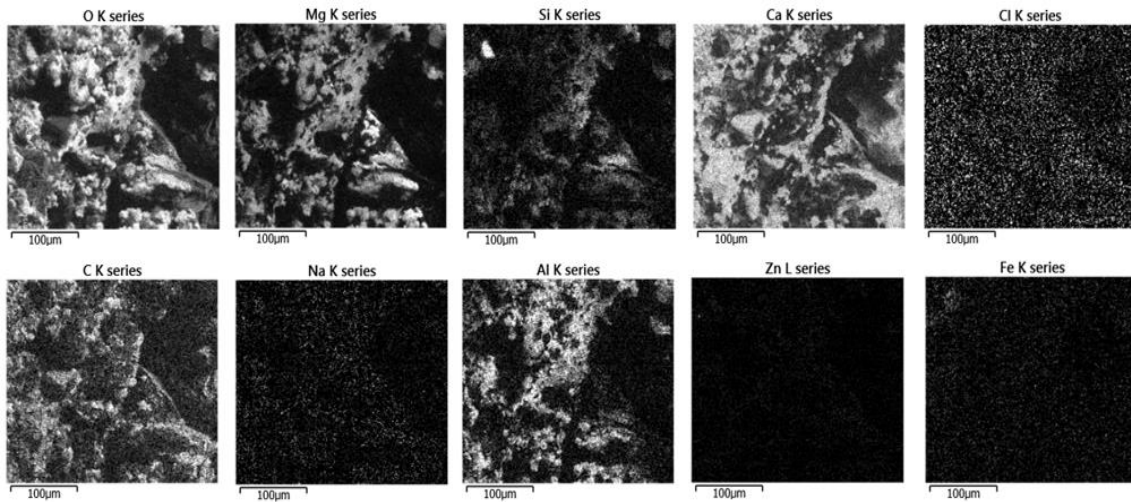


Figure 26: Elements found present in the efflorescence from hot bath samples

No sign of ASR was present, and thus it is assumed that the external cracking was caused by thermal expansion of the composite aggregate. This is further supported when looking at the coefficients of thermal expansion (CTE) of glass, epoxy, cement, and limestone shown in **Table 4**. It is clear that the glass and epoxy have a significant CTE than the cement and limestone, and therefore those stored in the hot bath may have experienced thermal cracking. To better understand the impact of thermal cracking, further work is needed to determine the true amount strain on the concrete samples by the thermal expansion of the composite aggregate.

Table 4: Coefficients of Thermal Expansion

Material	CTE (10⁻⁶ m/(m K))
Glass	22
Epoxy	25-36
Cement	6
Limestone	4.4

Regardless of what caused the external cracking shown on the samples stored in the hot bath, it is clear that it had a significant effect on both the compressive and tensile strength of each specimen. As the cracks spread in the hot bath samples throughout the study, the compressive strength decreased. This is concerning because the compressive strength should increase over time up to 482F (250C) [40]. Additionally, cylinders cured in the hot bath displayed significantly lower compressive and split tensile strength based on the ASTM C39 and ASTM C496 tests, respectively, compared to the fog room samples. Cylinders in hot bath showed an average compressive psi of 3,015 (20.8 MPa) and a split tensile psi of 366 (2.5 MPa) compared to the 6,318 (43.6 MPa) compressive psi and 578 psi (4.0 MPa) split tensile strength of the humidity room cylinders after 90 days. They correlate to a 52% reduction in compression strength and 37% reduction in split tensile strength from fog room to hot bath samples.

The samples stored in the hot bath do pose a concern when determining if using composite aggregate in concrete from wind turbine blades. However, those stored in the humidity showed promising results as the concrete cured over time. Similar to traditional concrete, the samples cured in the fog room saw compressive and tensile strength increases over time so long as appropriate moisture content and temperatures are available [41].

Effects of this expansion can also be noted in the ASTM C157 Shrinkage prisms test. All samples showed a positive length change during the time of this study ranging from 0.02% -

0.03% and 0.27%-0.33% in the fog and hot bath curing environments, respectively. The prisms stored in the hot bath displayed between 9 and 16.5 times greater change than the fog room prisms. Visible cracking was seen on the surface of the hot bath prisms, but there was no physical cracking of those stored in the fog room. Much of the cracking and expansion on the hot bath prisms is believed to be caused by thermal expansion similar to the effects seen in the cylinders used in the ASTM C39 compression and ASTM C496 split tensile tests. It is important to note that prisms stored in the fog room experienced positive length change as well. Expansion is not physically visible on the fog room cylinders used in the ASTM C39 and C496 tests, but based on the expansion seen in the fog room prisms it still thought to have occurred to a lesser extent.

It is unclear what caused this expansion since no sign of ASR was displayed when viewed under the SEM. It is possible that the sections viewed under the SEM did not contain ASR, but it could be present elsewhere in the samples which may have caused this expansion. If this is true, then the effects of expansion due to ASR are significantly lower than the thermal expansion, but it should still be taken into consideration. This expansion can have negative effect on the concrete similar to the cracking seen from thermal expansion [42]. If ASR does become an issue, the addition of fly ash can be used to reduce alkali-aggregate reaction if the replacement level is above a tested minimum [43].

The corrosion test was used to determine the effect concrete would have on the composite material. Prior to the experiment, it was expected that the acidic properties of a concrete environment would deteriorate the composite material. The deterioration was to be measured by mass loss over a 90 day curing cycle in a 160F (70C) calcium hydroxide bath. Samples were to

be weighed in a saturated surface dry state. The composite material was not expected to absorb any water.

After the initial weighing at seven days, an average weight gain of 0.83% was observed in the composite aggregate specimens. This is nearly double the 0.45% average weight increase seen in the limestone aggregate. The weight gain observed most likely came from water absorption. Over the next 83 days, the composite aggregate continued to absorb water ending with a 1.66% weight gain. Continued soaking after 90 days would be needed to determine if 1.66% is the complete saturation point or if the composite material would continue to absorb water. This water absorption is significant compared to the 0.49% seen in the limestone samples. However, previous studies have shown coarse limestone aggregate has higher absorption percentages of 2.2 [44] and 5.8 [45] for good quality limestone aggregate. The difference in absorption percentage in the limestones may be a result of the geographical location from which they were obtained. This has been seen before Kessler's absorption test with absorption percent as low as 0.04% and as high as 24.8% based on aggregate source location [46].

The sheared edges created during the aggregate production were likely the cause of this absorption. These sheared edges allow water to permanently saturate the composite material. This is further supported by the porosity claim made earlier. This test proved inconclusive in determining the deterioration and mass loss of the composite aggregate.

Although there are some areas that require further investigation, at this point it does seem plausible to use composite material from wind turbine blades as aggregate in concrete in selected applications such as pavement.

CHAPTER 3: ECONOMIC ANALYSIS

With the results of the experiment in favor of moving toward the use of composite aggregate, it is time to look at the next major piece on the puzzle. That is, using composite aggregate from wind turbines blades must make economic sense for this method to be a viable EOSL solution. The overall goal of this section is to determine the maximum allowable cost for producing one ton of composite aggregate. Before the cost could be justified, the demand must first be sought. The question arose, "If the composite aggregate were created, is there sufficient concrete demand to fully utilize the supply of composite material aggregate?" To answer this question, research was done to determine the quantity of aggregate currently used in Iowa. The study was limited to Iowa because transportation of the material over longer distances from where it originates will quickly become infeasible.

According to the Iowa Concrete Pavement Association, in 2015 there have been 292 miles (470 km) of concrete road placed as of October 30th 2015. It is predicted that approximately 290 miles (467 km) will be placed in 2016. On average, 300 miles (483 km) of concrete are laid annually. These roads have an average width of 9.33 yards (8.53 m) and depth of 9 inches (23 cm). This means that in a given year, approximately 1,232,500 yd³ (942,314 m³) of concrete will be used. Each cubic yard contains 1700 lb (771 kg) of limestone aggregate for a total of 2,095,250,000 lb (950,389,413 kg) of limestone aggregate annually.

Although this study used the assumption that 5% of blades will be recycled each year, the following model will allow the computation of the percent of total limestone aggregate replaced needed under other assumptions.

Equation 2:

$$\frac{\%BR * B_T * W_B * 1.4}{W_{LS}} = \% \text{ of total limestone aggregate replaced};$$

where %BR is the total percent of blades recycled, B_T is the total number of blades at a given time, W_B is the weight of a single turbine blade, 1.4 is the density conversion from composite material to limestone, and W_{LS} is the total amount of limestone aggregate used. The densities for crushed limestone and crushed composite material are 2,565 lb/yd³ and 1,826 lb/yd³ (1,522 kg/m³ and 1,083 kg/m³), respectively. Note the density for crushed limestone and crushed composite material used in this analysis is different than that of solid limestone and solid composite material used in the experiment. An exact density of crushed composite material was not known, thus the same ratio of solid limestone to crushed limestone (4,315 lb/yd³: 2,565 lb/yd³) was used to determine the density of the crushed composite material.

Currently, there are a total of 3,444 wind turbines consisting of 10,332 blades in Iowa [47]. If 5% of all blades are recycled each year, then in 2016 a total of 517 blades will be recycled. This is derived from a turbine lifespan of 20 years. At 12 tons per blade, 12,398,400 lb (5,623,820 kg) of composite material will be available in Iowa. The substitution of limestone aggregate to composite aggregate is done by volume due to the density differences of the two materials. In other words, 1 ton of composite aggregate is equal to 1.4 tons of limestone aggregate by volume. Thus, 12,398,400 lb (5,623,820 kg) of composite material is equivalent to 17,357,760 lb (7,873,347 kg) of limestone aggregate when substituted by volume. This shows a sufficient demand exists because if all the composite material were used as aggregate in concrete it would account for only 0.83% of the total limestone aggregate needed.

3.1 Assumptions

Now that a sufficient demand is identified, cost justification can be analyzed. This cost avoidance model assumes three things. First, the disassembly of the wind turbine is not included in the cost avoidance as it is required to disassemble the wind turbine regardless of EOSL

location. Disassembly includes both the removal of the blades from the turbine tower and cutting the blades into smaller sections. Second, a technology would be available to create the desired form of aggregate. There is no known way, currently, to create the desired geometry other than utilizing cutting and shearing operations similar to those performed in the experiment discussed later. However, the assumption is that the equipment would be created if there was a need for it. Third, it is assumed the composite aggregate will be created on site. This implies that the technology used to create the aggregate will be transported to the wind project site. This will allow for the finished aggregate to be transported directly to a concrete plant.

3.2 Cost avoidance for sending wind turbines to landfill

Almost none of the utility scale wind power projects in the US have been decommissioned. As a result, little is known about the full costs of decommissioning except that they will be substantial [48]. It is clear that in order for the composite material to be considered as aggregate, the cost avoidance from producing the aggregate must be greater than the sum of the costs of a blade removed from the tower and sent to its final EOSL location of a landfill. Giving the composite aggregate away, or paying someone to use it, may be a reasonable solution to avoid landfilling and the costs associated with it.

For this study, ten wind turbine decommissioning projects were analyzed to further understand the full cost of decommissioning. During this process, five major cost categories were established. These include preliminary costs, disassembly, blade processing, transportation, and landfill costs. Preliminary costs include items such as machinery set up and management costs. Disassembly costs account for labor, machinery, and tooling required to disassemble a turbine. A detailed breakdown of nine of the ten projects can be seen in **Table 5**.

Table 5: Decommissioning project cost per blade

Decommissioning Project breakdown Cost Per Blade							
Decommissioning Project	Preliminary Costs	Disassembly	Blade processing	Transportation to landfill Or	Landfill Cost	Total W/O Disassembly	Total Per Blade
Pinnacle Project (100% landfill) [49]	\$ 1,284	\$ 1,200		\$ 1,141	\$ 155	\$ 1,297	\$ 2,497
Monticello Hills Project [50]		\$ 7,350		\$ 2,070	\$ 825	\$ 2,895	\$ 10,245
Buffalo Ridge Farm II [51]					\$ 3,318	\$ 3,318	\$ 3,318
Bowers Mountain Project [52]	\$ 1,597	\$ 2,676	\$ 375	\$ 1,500	\$ 685	\$ 2,560	\$ 5,236
Sibley Wind Project [53]	\$ 2,500				\$ 5,000	\$ -	\$ 5,000
Community Wind South Farm [54]				\$ 4,063		\$ -	\$ 4,063
Canton Mountain Wind Project [55]	\$ 3,750	\$ 10,000	\$ 2,250			\$ 2,250	\$ 12,250
Suncor/Cedar Point [56]	\$ 618	\$ 4,303		\$ 4,990	\$ 1,000	\$ 5,990	\$ 10,293
Suncor/Adelaide [57]	\$ 618	\$ 4,303		\$ 4,990	\$ 1,000	\$ 5,990	\$ 10,293

The tenth is a second Pinnacle project. This project salvages 10% of blades and landfills the remaining 90%. These salvage values come from reselling blades at 25% of their original purchase price. The purpose of reselling these blades is to be used as spares [49]. Several assumptions were made in some cases due to a lack of information. In the case of the Bowers Mountain Project (BMP) and Canton Mountain Wind Project, it is assumed that the disassembly cost is broken up into eight components: Four tower sub-components, three blades, and the nacelle. A landfill tax of \$71 and \$45 per ton were used for the BMP and Suncor operations respectively.

Based on research regarding decommissioning projects for EOSL wind turbines, the total cost of blade processing, transportation, and landfiling range from \$108-\$499 per ton with an average of \$289 per ton of composite material. Looking only at the landfill cost, a cost avoidance of \$733 per 12 ton blade or \$61 per ton of composite material can be achieved based on **Table 2**. No scrap values of the tower, gearbox, or other components were taken into consideration in this model as they will be the same regardless of the blade disposition.

3.3 Cost avoidance for obtaining limestone course aggregate

In addition to the landfill cost avoidance, the cost avoidance for obtaining limestone course aggregate was calculated. Quotes for natural limestone aggregate from two Midwest

companies were obtained. Allied Manatts Group out of Charles City, Iowa, provided a quote of \$13.84 per ton, picked up on site. Burns & McDonnell's Chicago, Illinois branch stated their aggregate costs can be as high as \$25 per ton depending on delivery location within the state. If the substitution of limestone aggregate to composite aggregate were done by weight, \$13.84 and \$25 would be the cost avoidance. However, since the substitution is done by volume using the 1.4 limestone to composite density ratio, a cost avoidance between \$9.89 and \$17.85 per ton of composite aggregate produced is realized.

3.4 Cost avoidance for transporting aggregate

To determine the cost avoidance for transporting aggregate, three items were studied including: 1) the cost of transporting composite aggregate from a wind project to a concrete plant, 2) the cost avoidance of transporting limestone aggregate from a quarry to a concrete plant, and 3) the cost avoidance of transporting composite material to a landfill.

After a geographical review of the locations of quarries, concrete plants, and wind projects, the cost of transporting composite aggregate from a wind project to concrete plant were equally counteracted by the cost avoidance of transporting limestone aggregate from a quarry to a concrete plant. The abundance of the quarries and wind projects can be seen in **Figure 27**. The wind projects location were provided by the Iowa Wind Energy Association and landfills and quarries by the Iowa Department of Transportation. Additionally, according to the Iowa Pavement Concrete Association, each county in Iowa has its own concrete plant.

The cost avoidance of transporting composite material to a landfill cannot be ignored. Based on the large amounts of landfills in Iowa, a maximum travel distance of 50 miles (80.5 km) would be needed to take the blades from a wind project to a landfill. When shipping by truck, the average price per ton mile is 15.6 cents in 2015 according to the Congressional Budget

Office [58]. This would result in a maximum cost avoidance for transporting aggregate of \$7.80 per ton.

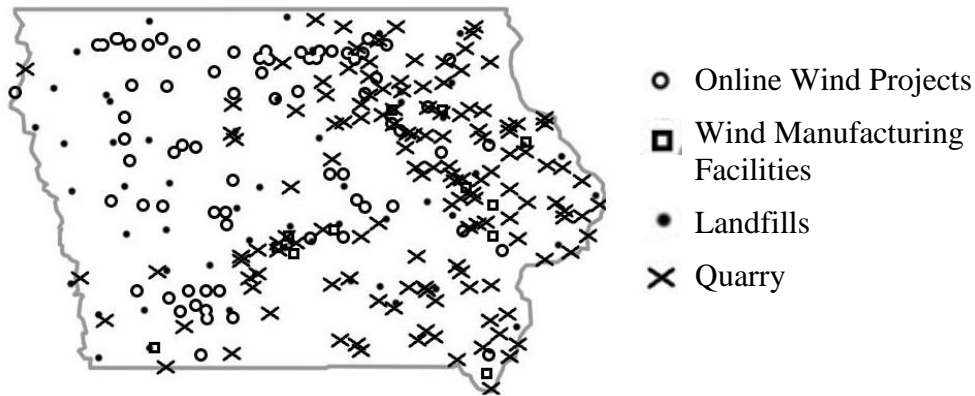


Figure 27: Distribution of online wind projects, wind manufacturing facilities, landfill, and quarries across Iowa

Cost of producing composite aggregate from wind turbines

Finally, a mobilization charge of \$1,000 for the machinery used to create the composite aggregate at the wind project site will be taken into consideration. This is a general estimation based on the cost to move the machinery from its stored location to the wind project site and back to its stored location. An average number of 35 wind turbines (or 105 blades) per wind project were calculated in Iowa based on the 99 wind projects with a total of 3,444 wind turbines. If 5% of the blades will be decommissioned each year, then approximately 5 blades will be removed per mobilization charge. This 5% is again derived from a turbine lifespan of 20 years. At 12 tons per blade, a cost of \$15.97 per ton of composite aggregate produced will be incurred.

Again, 5% of blades are assumed to be decommissioned each year. The following model will allow for the computation of a cost of producing aggregate from wind turbines based on other assumptions.

Equation 3:

$$\frac{C_{\text{Mobilization}}}{\frac{B_T}{WP_T} * \%BR * W_B} = \text{Cost of producing composite aggregate};$$

where $C_{\text{Mobilization}}$ is the mobilization charge for machinery used, B_T is the total number of blades at a given time, WP_T is the total number of wind projects, $\%BR$ is the total percent of blades recycled, and W_B is the weight of a single turbine blade.

The total cost avoidance includes the cost to landfill the blades, the cost of obtaining limestone aggregate, the cost to transport the composite material to a landfill, and the cost to produce composite aggregate. As seen in **Table 6**, the total cost avoidance of using composite aggregate in place of limestone aggregate is \$62.72. The cost of \$13.84 per ton of limestone aggregate from Allied Manatts Group was used in the calculation. In other words, the maximum allowable price to process one ton of composite aggregate is \$62.72. This value can provide guidance to the yet to be created equipment and industry that would efficiently process the spent blades into useful aggregate. Additionally, any post processing, coatings, or even funds to pay concrete suppliers to use the composite aggregate may be part of this \$62.72.

Table 6: Cost avoidance per ton of composite aggregate produced

Total Cost avoidance for producing 1 ton of composite aggregate	
Landfill	\$ 61.00
Limestone aggregate	\$ 9.89
Transporting composite aggregate to landfill	\$ 7.80
Machinery mobilization cost	\$ (15.97)
Total cost avoidance	\$ 62.72

CHAPTER 4: ENVIRONMENTAL IMPACT

4.1 Recycling vs landfilling vs incineration of composite material

Pressure is being placed on industry from all sides to reduce the production of waste and steer towards environmentally friendly methods of production and material disposal. The same holds true for wind energy, which leads us to the final step in determining the feasibility of using composite material from wind turbine blades as aggregate in concrete. The idea of wind energy is thought to be a green alternative to the production of energy when compared to coal or oil; however, the impact of the non-biodegradable fiberglass used in the construction of wind turbines blades which eventually must be disposed of is often overlooked. There are currently three types of disposal for EOSL wind turbine blades: incineration, landfill, or recycling. Incineration leaves behind 60% of the material (e.g. the glass fiber) as ash which must be disposed of, and the inorganic glass fibers may lead to emissions of hazardous flue gasses when cleaning dust filter devices [7]. Another study further supports this claim by stating that incineration can only recover the calorific value of materials provided by the organic fraction within fiber reinforced composites. The glass fibers are considered incombustible. Through his work, Cherrington shows the average calorific values of 18.1, 13.6, 7.7, 0, and 15.4 MJ/lb (40, 30, 17, 0, and 34 MJ/kg) were found of polyester, epoxy, polyvinyl chloride, glass fibers, and carbon fibers found in a wind turbine blade respectively [13]. Additionally, emissions from this process is still a concern. Although it is a concern, similar issues have been seen when recycling fiberglass-based epoxy printed circuit boards. These issues are addressed by using afterburners [59].

As regulations regarding landfills become more and more strict, several developed countries such as Germany have already enforced a landfill ban on municipal solid waste causing

wind turbine blades to find an alternative EOSL destination [13]. With regulations like the one seen in Germany expected to appear in the US and around the world, finding a more efficient way to deal with the deconstruction is crucial to the ability to recycle this material. Several mechanical operations alternatives include hammer milling, grinding, crushing or shredding. Similar to the vapor emissions of incineration, dust emissions should be minimized to ensure that all environmental, health, and safety requirements are met [24].

4.2 Life Cycle Analysis

A life cycle analysis (LCA) was conducted to determine the comparison between using natural limestone aggregate while landfilling the turbine blades and using the turbine blades as composite aggregate. To determine the effects of utilizing composite aggregate in place of natural aggregate, a previous LCA was analyzed. This LCA was conducted on aggregates and determined between 5.35 lb (2.43 kg) and 9.11 lb (4.14 kg) of CO₂ was emitted per 2,205 lb (1000 KG) of aggregate produced [60]. Using composite aggregate in place of limestone aggregate gives an avoidance of 1.4 tons (0.1.3 tonne) of limestone aggregate per ton of composite aggregate produced. This equates to between 3.98 (1.81 kg) and 6.77 lb (3.07 kg) reduction in CO₂ emissions per ton of composite aggregate produced.

Coupled with emissions reduction from creating the natural aggregate, the avoidance of landfilling the composite material was calculated. With wind energy being one of the fastest growing renewable energy sources in the world, issues of landfill capacity increase as the number of blades needed to be decommissioned increases. These issues come from the inorganic components of a turbine blade. The fiberglass in a wind blade is made of 50% resin and 50% glass. The resin is organic while the glass is not. Concerns with the inorganic glass arise due to its non-biodegradability and landfill capacity. The organic material raises concern as well. Many

organic materials are broken down in landfills by microorganisms leading to the emissions of gas and leachate [16]. Emissions in this study were only calculated based on the organic material found in the blade.

Emissions avoidance can be seen for the composite material that will not be landfilled due to the recycling processes. These emissions are expected from the organic resin in the blades when landfilled and the transportation of the composite aggregate to the landfill. Similar to the economic analysis, the composite material was expected to travel a maximum of 50 miles (80.5 km) to a landfill. The emissions avoidance from transporting the composite material to the landfill equate to 17.2 lb (7.8 kg). Once the composite material is in the landfill, a total of 2.7 lb (1.2 kg) per ton of composite material is expected. The total emissions avoidance for landfilling the composite material is 19.9 lb (9.0 kg) from both the transportation and storage of the composite material. An LCA of production of composite aggregate was also taken into consideration during this environmental impact study. The disassembly and cutting of the blades to smaller, more transportable sizes was also disregarded since it is required in every EOSL scenario. This LCA assumes a chipper-like machine would be used to chip the blades into the useable composite aggregate size and shape. To estimate the impact of this machine in the LCA, the machine specifications were modeled after Vermeer's Horizontal Grinder 4000 (HG4000) [61]. From here, the composite aggregate production emissions were calculated. This was broken into two components. First the transportation of the chipping machine to the wind project site. For this, a maximum travel distance of 150 miles (241 km) was used. Again, an average number of five blades will be processed per mobilization similar to the economic analysis. The second component was the use of the chipping machine to produce the composite aggregate. According to the HG4000 specifications, the maximum fuel consumption of 25.4 gph (96.1 lph) was used.

CO₂ emissions of 19.0 lb (8.6) and 2.5 lb (1.1 kg) per ton of composite aggregate produced were found for the transportation and use of the chipping machine respectively.

The total emission reduction from using composite aggregate as opposed to limestone is 23.8 lb (10.8 kg) of CO₂. When compared to the total emission production of using composite aggregate as opposed to limestone is, 21.5 lb (9.8 kg) of CO₂, a total CO₂ emissions avoidance of 2.3 lb (1.0 kg) is seen per ton of composite aggregate produced. Avoidance of CO₂ emissions found through this evaluation was 20.0 lb per ton of composite aggregate produced. This number is based on five blades being processed per location, similar to that seen in the economic analysis. As the number of blades processed per location increases the total emission production will decrease per ton of composite material based on the emissions caused by the mobilization of the machinery to produce the aggregate. This method favors recycling the composite material from wind turbine blades as aggregate in concrete. A summary of the CO₂ emissions can be seen in **Table 7**.

Table7: CO₂ emission per ton of composite aggregate produced

CO ₂ avoidance or production	lb (kg)
Avoidance from Limestone	4.0 (1.8)
Avoidance from landfilling composite	2.7 (1.2)
Avoidance from transporting composite to landfill	17.2 (7.8)
Production from transportation of chipping machine	19.0 (8.6)
Production from use of chipping machine	2.5 (1.1)
Total emission reduction	23.8 (10.8)
Total emission production	21.5 (9.8)
Total emission avoidance	2.3 (1.0)

In addition to CO₂ emissions, regular aggregate is created by blasting which creates other pollutants as well. Controlling these emissions for natural aggregate creation usually depends on the use of water trucks, sweepers, and chemical applications on haul roads; control of vehicle speed; and construction of windbreaks and plantings [62]. Other concerns with the creation of

natural aggregate have been raised in the past regarding ground vibrations, noise, and flyrock. However, technology of rock blasting is highly developed and the environmental impacts should be negligible [63].

CHAPTER 5: SUMMARY AND CONCLUSIONS

5.1 Summary

The landfilling of wind turbine blades due to sub-optimal recycling methods will continue to pose a problem as more and more wind turbines will need to be decommissioned each year. Finding alternative end-of-service-life locations for the blades is a necessity with wind energy being one of the fastest growing energy sources in the world. Several options have been explored in the past including mechanical and thermal recycling. Both these solutions have encountered issues with changes in physical properties and incomplete disposal. One possible outlet for the blades is using the composite material as aggregate in concrete.

The results of this study show some cases which favor the use of composite material from wind turbine blades as aggregate in concrete. Simultaneously, several issues were found throughout these studies that threaten the practicality of composite aggregate for this purpose. The specific conclusions of this study are summarized as below.

1. The experiment strength test, ASTM C39 compression test and ASTM C496 split tensile test, results of this study were split. Those stored in the hot bath displayed values not suitable for use. With no signs of alkali-silica reaction occurring between the fiberglass and cement, thermal expansion issues were identified as the reason for the reduced strength found in these samples. Those cured in the 100% humidity environment yielded results similar to that of regular concrete containing no composite aggregate. The scanning electron microscopic evaluation supported the theory of poor bonding along the smooth edges of the composite aggregate while creating more sufficient bonds along the sheared edges. A decrease in compressive and tensile strength is also attributed to the lack of bonding along the smooth edges seen amongst the samples.

2. The corrosion test proved inconclusive, but shone a light on issues that may arise due to water absorption in freeze-thaw conditions. Additionally, samples stored in both curing environments showed signs of expansion when measured on the ASTM C157 shrinkage prism test. While the hot bath expansion was attributed to thermal expansion, the cause of humidity samples expansion was unclear. Although the SEM showed no signs of ASR, the expansion seen in the humidity environment may hint towards ASR being present in other areas of the samples.
3. Using the composite material as aggregate in concrete makes economic sense if it can be produced for less than \$62.72 per ton. Concerns arise when looking at the ability to produce the desired geometry efficiently. A manual process does not suffice for this operation.
4. At its current state, an emissions avoidance of 2.3 lb (1.0 kg) of CO₂ emissions per ton of composite aggregate seen from this recycling process favors recycling wind blades as aggregate in concrete. This is further supported by the 50% of fiberglass in the blades comprised of inorganic material raising concerns of landfills reaching capacity. This issue is only inflated as wind energy grows and the number of wind blades to be decommissioned at a given time increases.

5.2 Conclusions

The results of this study show that the use of the composite material from wind turbine blades as aggregate in concrete is feasible under certain conditions. To fully understand these conditions, additional research must occur. A freeze-thaw cycle is needed to determine the effects of thermal contraction and absorption properties of the composite material. Additionally, a viable solution to create the composite aggregate in a more economic manner is required.

Finally, the effects of irregular shaped composite aggregate should be explored to determine if it would enhance overall strength of concrete containing composite aggregate.

REFERENCES

1. World Wind Energy Association. *New Record In Worldwide Wind Installations*. *Wwindea.org*. N.p., 5 Feb. 2015. "Research Note Outline on Recycling Wind Turbines Blades."
2. Hoeven, Maria Van Der. *Technology Roadmap: Wind Energy*. Publication. Paris: International Energy Agency, 2013.
3. Vision, Wind. *A New Era for Wind Power in the United States*. Technical report, US Department of Energy, Washington, DC, 2015.
4. Zayas, Jose, Michael Derby, Patrick Gilman, Shreyas Ananthan, Eric Lantz, Jason Cotrell, Fredric Beck, and Richard Tusing. 2015. *Enabling Wind Power Nationwide*. U.S. Department of Energy.
5. Sritharan, Sri. "Wind turbine towers." *PCI Journal* (2015).
6. Ortegon, Katherine, Loring F. Nies, and John W. Sutherland. "Preparing for end of service life of wind turbines." *Journal of Cleaner Production* 39 (2013): 191-199.
7. Larsen, Kari. "Recycling wind turbine blades." *Renewable energy focus* 9.7 (2009): 70-73.
8. "Wind Power Facts." *Iowa Wind Energy Association*. Iowa Wind Energy Association
9. Ozment, S., Tremwell, T., 2007. Transportation management in the wind industry: problems and solutions facing the shipment of oversized products in the supply chain. 28, DOI: SCMR-WP025-1007.
10. Ancona, Dan, and Jim McVeigh. "Wind turbine-materials and manufacturing fact sheet." Princeton Energy Resources International, LLC (2001).
11. Vestas Wind Systems A/S of the Danish Elsam Engineering, trans. Life Cycle Assessment of Offshore and Onshore Sited Wind Farms. Rep. no. 200128. N.p.: Elsam Engineering A/S, 2004.
12. D'Souza, Neil, Erhi Gbegbaje-Das, and Peter Shonfield, Dr. Life Cycle Assessment of Electricity Production from a V112 Turbine Wind Plant. Rep. Copenhagen: PE North West Europe ApS, 2001.
13. Cherrington, R., V. Goodship, J. Meredith, B.m. Wood, S.r. Coles, A. Vuillaume, A. Feito-Boirac, F. Spee, and K. Kirwan. "Producer Responsibility: Defining the Incentive for Recycling Composite Wind Turbine Blades in Europe." *Energy Policy* 47 (2012)): 13-21
14. Milanese, Alice. "Recyclability of wind turbines, current and future: technical, economic and environmental." (2009).
15. Carra, Joseph S., and Raffaello Cossu. "International perspectives on municipal solid wastes and sanitary landfilling." (1990).
16. El-Fadel, Mutasem, Angelos N. Findikakis, and James O. Leckie. "Environmental impacts of solid waste landfilling." *Journal of environmental management* 50.1 (1997): 1-25.
17. Cunliffe, Adrian M., and Paul T. Williams. "Characterisation of products from the recycling of glass fibre reinforced polyester waste by pyrolysis." *Fuel* 82.18 (2003): 2223-2230.
18. Åkesson, Dan, et al. "Microwave pyrolysis as a method of recycling glass fibre from used blades of wind turbines." *Journal of Reinforced Plastics and Composites* 31.17 (2012): 1136-1142.

19. Lester, Edward, et al. "Microwave heating as a means for carbon fibre recovery from polymer composites: a technical feasibility study." *Materials Research Bulletin* 39.10 (2004): 1549-1556.
20. Pickering, S. J., et al. "A fluidised-bed process for the recovery of glass fibres from scrap thermoset composites." *Composites Science and Technology* 60.4 (2000): 509-523.
21. Pickering, S. J. "Recycling technologies for thermoset composite materials—current status." *Composites Part A: Applied Science and Manufacturing* 37.8 (2006): 1206-1215.
22. Scheirs, John. "Polymer recycling: science, technology and applications." John! Wiley & Sons Ltd, Journals, Baffins Lane, Chichester, Sussex PO 19 1 UD, UK, 1998. 591 (1998).
23. Ewea.org. The European Wind Energy Association, n.d. Web. <http://www.ewea.org/fileadmin/files/our-activities/policy-issues/environment/research_note_recycling_WT_blades.pdf>.
24. "Disused Rotor Blades Can Now Be Utilized in Cement Production." Holcim. Holcim 2015, n.d. Web. 04 Dec. 2015. <<http://www.holcim.com/referenceprojects/disused-rotor-blades-can-now-be-utilized-in-cement-production.html>>.
25. Schmidl, Erwin, Dr. Recycling of Fibre - Reinforced Plastics Using The Example of Rotor Blades. ISWA World Congress 2010 Review and Presentation Papers. Holcim: Geocycle, 2010.
26. Hofmeister, Michael. Recycling Turbine Blade Composites: Concrete Aggregate and Reinforcement. Tech. N.p.: n.p., 2012.
27. Kim, Sunghwan, et al. "Comparative performance of concrete pavements with recycled concrete aggregate (RCA) and virgin aggregate subbases." *Reston, VA: ASCE Proceedings of the First Transportation and Development Institute Congress; March 13-16, 2011, Chicago, Illinois/ d 20110000*. American Society of Civil Engineers, 2011.
28. Rahim, Nur Liza, Shamshinar Sallehuddin, Norlia Mohamad Ibrahim, Roshazita Che Amat, and Mohd Faizal Ab Jalil. "Use of Plastic Waste (High Density Polyethylene) in Concrete Mixture as Aggregate Replacement." *AMR Advanced Materials Research* 701 (2013): 265-69.
29. Maier, Patrick L., and Stephan A. Durham. "Beneficial use of recycled materials in concrete mixtures." *Construction and Building Materials* 29 (2012): 428-437.
30. de Brito, Jorge, and Nabajyoti Saikia. "Use of Industrial Waste as Aggregate: Properties of Concrete." *Recycled Aggregate in Concrete*. Springer London, 2013. 115-228.
31. Shi, Caijun, and Keren Zheng. "A review on the use of waste glasses in the production of cement and concrete." *Resources, Conservation and Recycling* 52.2 (2007): 234-247.
32. Topcu, Ilker Bekir, and Mehmet Canbaz. "Properties of concrete containing waste glass." *Cement and Concrete Research* 34.2 (2004): 267-274.
33. Etxeberria, Miren, et al. "Influence of amount of recycled coarse aggregates and production process on properties of recycled aggregate concrete." *Cement and concrete research* 37.5 (2007): 735-742.
34. Asokan, Pappu, Mohamed Osmani, and Andrew DF Price. "Assessing the recycling potential of glass fibre reinforced plastic waste in concrete and cement composites." *Journal of Cleaner Production* 17.9 (2009): 821-829.
35. de Castro, Sara, and Jorge de Brito. "Evaluation of the durability of concrete made with crushed glass aggregates." *Journal of Cleaner Production* 41 (2013): 7-14.

36. Piotrowska, E., Y. Malecot, and Y. Ke. "Experimental investigation of the effect of coarse aggregate shape and composition on concrete triaxial behavior." *Mechanics of Materials* 79 (2014): 45-57.
37. Johnston, C. D. "Waste glass as coarse aggregate for concrete." *ASTM Journal of Testing and Evaluation* 2.5 (1974).
38. Farny, James A., and Steven H. Kosmatka. *Diagnosis and control of alkali-aggregate reactions in concrete*. Portland Cement Association, 1997
39. Rajabipour, Farshad, et al. "Alkali-silica reaction: Current understanding of the reaction mechanisms and the knowledge gaps." *Cement and Concrete Research* 76 (2015): 130-146.
40. Ikponmwosa, Efe E., and Musbau A. Salau. "Effect of heat on laterised concrete." *Maejo International Journal of Science and Technology* 4.1 (2010): 33-42.
41. Nawy, Edward G., ed. *Concrete construction engineering handbook*. CRC press, 2008.
42. Radwan, Ramy Z., et al. "The Impact of Expansion due to Alkali-Carbonate Reaction on Engineering Properties of Concrete." *1st International/1st Engineering Mechanics and Materials Specialty Conference* "Proceedings of the Annual Conference of the Canadian Society for Civil Engineering, St. John's NL, Canada. 2009.
43. Dunstan, E. R. "The effect of fly ash on concrete alkali-aggregate reaction." *Cement, Concrete and Aggregates* 3.2 (1981): 101-104.
44. Maslehuddin, M., et al. "Comparison of properties of steel slag and crushed limestone aggregate concretes." *Construction and building materials* 17.2 (2003): 105-112.
45. Solis-Carcaño, Rómel, and Eric I. Moreno. "Evaluation of concrete made with crushed limestone aggregate based on ultrasonic pulse velocity." *Construction and Building Materials* 22.6 (2008): 1225-1231.
46. Kessler, Daniel William, and William Hume Sligh. *Physical properties of the principal commercial limestones used for building construction in the United States*. Vol. 349. US Govt. Print. Off., 1927.
47. American Wind Energy Association. *Wind Was Largest Source of New Electricity in 2014, Congress Still Must Provide Long-term Policy Certainty*. Awea.org. 1996-2015 American Wind Energy Association, 5 Mar. 2015.
48. Ferrell, Shannon L., and Eric A. Devuyt. "Decommissioning Wind Energy Projects: An Economic and Political Analysis." *Energy Policy* 53 (2013): 105-13
49. Hewson, R., and T. Giustino. *Decommissioning Study for the Pinnacle Wind Power Project*. Rep. San Diego: Gerrad Hansan America, 2011.
50. "Knauth's Analysis of cost to decommission turbines. Public commentary on the Ridgeline Energy LLC Monticello Hills Application." Knauth (2011). Web. Construction and Demolition Waste." *Green Energy and Technology* (2013
51. Renewables, Iberdrola. "Buffalo ridge II wind farm decommissioning report." (2008).
52. *Section 29 Decommissioning Plan*. Rep. Vol. 29. N.p.: Patriot Renewables Canton Mountain Wind, 2011.
53. WESCO-Sibley SPV, LLC. "Decommissioning Plan Sibley Wind Project." Decommissioning Plan Report. (n.d.)
54. "Decommissioning and Site Restoration Plan Community Wind South Wind Farm." Zephyr Wind, LLC (n.d.).
55. Patriot Renewables. "Section 29 Decommissioning Plan." Canton Mountain Wind Project LLC (n.d.).

56. Stantec Consulting Ltd. "Suncor Energy Cedar Point Wind Power Project." Decommissioning Plan Report. (2013).
57. *Suncor Energy Adelaide Wind Power Project Decommissioning Plan Report*. Rep. no. 160960710. Guelph: Stantec Consulting, 2012.
58. Austin, David. "Pricing Freight Transport to Account for External Costs." (2015).
59. Goosey, Martin and Rod Kellner, (2003) "Recycling technologies for the treatment of end of life printed circuit boards (PCBs)", *Circuit World*, Vol. 29 Iss: 3, pp.33 - 37
60. Korre, A., and S. Durucan. "Life Cycle Assessment of Aggregates, EVA025–Final Report: Aggregates Industry Life Cycle Assessment Model: Modelling Tools and Case Studies." *Waste and Resources Action Programme, Oxon* (2009).
61. "HG4000 Horizontal Grinder." *Vermeer*. Vermeer Corporation, n.d. Web. <http://www2.vermeer.com/vermeer/NA/en/N/equipment/horizontal_grinders/hg4000>.
62. Langer, W. N., 2001, Environmental impacts of mining natural aggregate, in Bon, R. L., Riordan, R. F., Tripp, B. T., and Krukowski, S. T., eds., Proc. 35th Forum on the Geology of Industrial Minerals—The Intermountain West Forum: Utah Geol. Survey Misc. Publ. 01–2, p. 127–138.
63. Drew, Lawrence J., William H. Langer, and Janet S. Sachs. "Environmentalism and natural aggregate mining." *Natural Resources Research* 11.1 (2002): 19-28.

APPENDIX A: RAW DATA

Table A1: Compressive strength of pretest cylinders when determining aggregate size

Sample	ASTM C39 Compression test							
	Control - No composite		1/2" composite aggregate		50-50 composite aggregate		1" Composite aggregate	
	LBS	PSI	LBS	PSI	LBS	PSI	LBS	PSI
1	73,145	5,821	39,060	3,108	39,700	3,159	40,135	3,194
2	72,095	5,737	39,215	3,121	42,170	3,356	42,480	3,380
3	73,920	5,882	43,805	3,486	39,225	3,121	40,985	3,262
Mean	73,053	5,813	40,693	3,238	40,365	3,212	41,200	3,279
Std. Dev	916	73	2,696	215	1,581	126	1,187	94

Table A2: Compressive strength of pretest cylinders when determining aggregate volume

Sample	ASTM C39 Compression test							
	25% Composite Aggregate		37.5% Composite Aggregate		50% Composite Aggregate		Control	
	LBS	PSI	LBS	PSI	LBS	PSI	LBS	PSI
1	57,570	4,581	46,355	3,689	42,345	3,370	73,145	5,821
2	56,175	4,475	47,135	3,751	37,480	2,982	72,095	5,737
3	57,025	4,538	43,515	3,463	41,275	3,285	73,920	5,882
Mean	56,923	4,531	45,668	3,634	40,367	3,212	73,053	5,813
Std. Dev	703	53	1,905	152	2,557	204	916	73

Table A3: Weights from composite aggregate corrosion test

Sampel #	Corrosion Test Fiberglass Units in grams															
	1		2		3		4		5		6		7		8	
Original Weight	8.003		9.45		14.764		7.821		9.435		7.467		8.363		10.129	
7 days	8.109	1.31%	9.565	1.20%	14.867	0.69%	7.863	0.53%	9.5	0.68%	7.521	0.72%	8.43	0.79%	10.201	0.71%
28 days	8.128	1.54%	9.576	1.32%	14.894	0.87%	7.886	0.82%	9.523	0.92%	7.533	0.86%	8.445	0.97%	10.225	0.94%
90 days	8.17	2.04%	9.64	1.97%	14.998	1.56%	7.938	1.47%	9.587	1.59%	7.58	1.49%	8.505	1.67%	10.282	1.49%

Table A4: Weights from limestone aggregate corrosion test

Sampel #	Corrosion Test Limestone Units in grams															
	1		2		3		4		5		6		7		8	
Original Weight	7.973		10.164		6.751		8.708		4.405		4.647		6.037		7.991	
7 days	8.014	0.51%	10.174	0.10%	6.77	0.28%	8.754	0.53%	4.444	0.88%	4.675	0.60%	6.052	0.25%	8.025	0.42%
28 days	8.014	0.51%	10.174	0.10%	6.77	0.28%	8.758	0.57%	4.448	0.97%	4.676	0.62%	6.054	0.28%	8.033	0.52%
90 days	8.018	0.56%	10.178	0.14%	6.772	0.31%	8.763	0.63%	4.445	0.90%	4.674	0.58%	6.054	0.28%	8.032	0.51%